AFRL-RX-WP-TP-2012-0353

IN SITU ESTIMATION OF APPLIED BIAXIAL LOADS WITH LAMB WAVES (PREPRINT)

Fan Shi, Jennifer E. Michaels, and Sang Jun Lee

Georgia Institute of Technology

July 2012
Interim

AIR FORCE RESEARCH LABORATORY
MATERIALS AND MANUFACTURING DIRECTORATE
WRIGHT-PATTERSON AIR FORCE BASE, OH 45433-7750
AIR FORCE MATERIEL COMMAND
UNITED STATES AIR FORCE

REPORT DOCUMENTATION PAGE

Form Approved
OMB No. 0704-0188

1. REPORT DATE *(DD-MM-YY)*	2. REPORT TYPE	3. DATES COVERED *(From - To)*
July 2012	Technical Paper	1 June 2012 – 1 July 2012

4. TITLE AND SUBTITLE
IN SITU ESTIMATION OF APPLIED BIAXIAL LOADS WITH LAMB WAVES (PREPRINT)

5a. CONTRACT NUMBER
FA8650-09-C-5206

5b. GRANT NUMBER

5c. PROGRAM ELEMENT NUMBER
62102F

6. AUTHOR(S)
Fan Shi, Jennifer E. Michaels, and Sang Jun Lee

5d. PROJECT NUMBER
4349

5e. TASK NUMBER
41

5f. WORK UNIT NUMBER
LP106300

7. PERFORMING ORGANIZATION NAME(S) AND ADDRESS(ES)
Georgia Institute of Technology
Georgia Tech Research Group
505 10th Street NW
Atlanta, GA 30332

8. PERFORMING ORGANIZATION REPORT NUMBER
AFRL-RX-WP-TP-2012-0353

9. SPONSORING/MONITORING AGENCY NAME(S) AND ADDRESS(ES)
Air Force Research Laboratory
Materials and Manufacturing Directorate
Wright-Patterson Air Force Base, OH 45433-7750
Air Force Materiel Command
United States Air Force

10. SPONSORING/MONITORING AGENCY ACRONYM(S)
AFRL/RXCA

11. SPONSORING/MONITORING AGENCY REPORT NUMBER(S)
AFRL-RX-WP-TP-2012-0353

12. DISTRIBUTION/AVAILABILITY STATEMENT
Approved for public release; distribution unlimited. Preprint to be submitted to Journal of the Acoustical Society of America.

13. SUPPLEMENTARY NOTES
This work was funded in whole or in part by Department of Air Force contract FA8650-09-C-5206. The U.S. Government has for itself and others acting on its behalf an unlimited, paid-up, nonexclusive, irrevocable worldwide license to use, modify, reproduce, release, perform, display, or disclose the work by or on behalf of the U.S. Government. PA Case Number and clearance date: 88ABW-2012-0773, 14 February 2012. This document contains

14. ABSTRACT
Spatially distributed arrays of piezoelectric discs are being applied to monitor the integrity of critical metallic structures using guided elastic waves. These transducers are subjected to in situ operational and environmental conditions, and stress variations are of particular importance because of their cumulative effects on the fatigue life of the structures. Waves propagating between array elements are directly affected by applied loads because of both dimensional changes and the acoustoelastic effect. In particular, changes in phase velocity are a function of the direction of propagation for a particular Lamb wave mode and frequency. This paper shows from numerical solutions of the acoustoelastic wave equation that it is possible to decouple the effects of a homogeneous biaxial stress into its two principal components. As a consequence of this decoupling combined with material isotropy, the acoustoelastic response of guided waves is described by only two constants, both of which can be determined from a single uniaxial loading experiment.

15. SUBJECT TERMS
guided waves, acoustoelasticity, applied loads

16. SECURITY CLASSIFICATION OF:			17. LIMITATION OF ABSTRACT:	NUMBER OF PAGES	19a. NAME OF RESPONSIBLE PERSON (Monitor)
a. REPORT	b. ABSTRACT	c. THIS PAGE			Charles Buynak
Unclassified	Unclassified	Unclassified	SAR	26	19b. TELEPHONE NUMBER *(Include Area Code)* N/A

In Situ Estimation of Applied Biaxial Loads with Lamb Waves

Fan Shi, Jennifer E. Michaels and Sang Jun Lee

School of Electrical and Computer Engineering, Georgia Institute of Technology,
Atlanta, GA, USA 30332-0250

ABSTRACT. Spatially distributed arrays of piezoelectric discs are being applied to monitor the integrity of critical metallic structures using guided elastic waves. These transducers are subjected to *in situ* operational and environmental conditions, and stress variations are of particular importance because of their cumulative effects on the fatigue life of the structures. Waves propagating between array elements are directly affected by applied loads because of both dimensional changes and the acoustoelastic effect. In particular, changes in phase velocity are a function of the direction of propagation for a particular Lamb wave mode and frequency. This paper shows from numerical solutions of the acoustoelastic wave equation that it is possible to decouple the effects of a homogeneous biaxial stress into its two principal components. As a consequence of this decoupling combined with material isotropy, the acoustoelastic response of guided waves is described by only two constants, both of which can be determined from a single uniaxial loading experiment. Furthermore, an arbitrary biaxial load can be estimated from time shifts of signals recorded between array elements. The method is validated experimentally by recording load-dependent data during fatigue tests. The additional impact of interference between guided waves and opened cracks is mitigated by removal of data from some transducer pairs. Results show that applied stresses can be successfully recovered from the measured changes in guided wave signals even in the presence of significant fatigue damage.

Keywords: Guided Waves, Acoustoelasticity, Applied Loads

I. INTRODUCTION

Metallic plate-like structures are widely used in the construction of engineering structures such as are common for aerospace, automotive and civil applications. The fatigue life of these structures is critical for the safety of users. However, vibrations and large deflections during normal operation cause stresses that cause damage and limit fatigue life. Thus, *in situ* measurements of stresses are important to ensure the quality of metallic plate-like materials, and it is advantageous to utilize the guided wave transducers that are already in place for damage detection. Furthermore, recording data during variable applied stress conditions is useful for selecting appropriate baseline data for various structural health monitoring methods using guided waves [1].

Most nondestructive evaluation techniques to estimate stresses are based upon acoustoelastic theory [2], which refers to the variation of ultrasonic wave speeds with applied or residual stresses. Pao *et al*. [3, 4] provided a detailed summary of acoustoelastic theory of bulk waves, and derived several formulae to calculate residual stresses, including acoustoelastic birefringence techniques. Degtyar and Rokhlin [5] also developed an approach to simultaneously calculate stresses and stress-dependent elastic constants by inverting the angle dependence of phase velocities as measured with bulk waves.

When stresses are concentrated near the surface, it is more appropriate to employ surface waves for their measurement. For example, noncontact acoustic microscopy was applied to measure acoustoelastic constants and residual stresses via surface waves [6]. Duquennoy *et al*. [7, 8] derived theoretical formulae to calculate surface wave acoustoelastic constants directly from 2nd and 3rd order elastic constants measured using bulk waves. Junge *et al*. [9] introduced a method

to recover stresses from the polarization of surface waves instead of wave speed changes because polarization is more sensitive to applied stresses than relative phase velocities. Both bulk and surface wave methods that rely upon absolute measurements of velocity are adversely affected by anisotropic texture effects and surface roughness, although differential methods that measure changes in wave speed from an unstressed reference state are much less affected.

Acoustoelastic effects have also been investigated for propagation of guided waves in rod-like structures supporting a single direction of propagation. In the domain of prestressed tendons or cable stays, Rizzo and Scalea [10] experimentally investigated the effects of frequency on acoustoelastic sensitivity in a bar to enable selecting a frequency that maximizes the sensitivity of the stress monitoring technique. Chen and Wilcox [11] developed a finite element technique for modeling the dispersion relationship of guided wave propagation in prestressed cable-like or rail-like structures, and compared it with an Euler-Bernoulli beam model regarding the sensitivity of certain modes and frequencies to applied loads. Loveday and Wilcox [12] used the semi-analytical finite element method to reduce the complexity of the 3-D finite element formulation into discretization of a 2-D mesh, and analyzed measurement of axial loads in rail-like structures. Chaki and Bourse [13] developed a method to optimize the measurement of uniform axial stress in steel strands by taking acoustoelastic and geometrical considerations into account. Bartoli *et al*. [14] proposed a methodology using nonlinear ultrasonic waves to monitor prestress levels in tendons by measuring the nonlinear parameter β as a function of applied stresses.

Less research has been focused on guided waves in plate-like structures because of the added complexity of considering both 2-D applied stresses (i.e., biaxial vs. uniaxial) and 2-D guided wave propagation. Desmet *et al*. [15] theoretically determined guided wave dispersion curves for stressed polymer foils and compared them with experimental results, but neglected third-order elastic constants due to the small values of stress applied. Lematre *et al*. [16] studied the dispersion characteristics of Lamb wave propagation in a piezoelectric plate with a uniform applied stress, but did not report results for either biaxial loads or propagation at an angle to a uniaxial load. Zagrai *et al*. [17] experimentally measured acoustoelastic guided wave signal responses for wave propagation parallel and perpendicular to applied uniaxial stresses.

To the best knowledge of the authors, published methods using Lamb waves to monitor stress levels consider only guided waves propagating parallel or perpendicular to the direction of an applied, uniaxial stress. However, for operation under realistic conditions, near-homogeneous stresses in plate-like structures are in general biaxial with unknown principal directions. The motivation of this paper is to develop a strategy for in situ estimation of a general homogeneous, biaxial stress field using a spatially distributed array of guided wave sensors, which is an extension of work reported in [18].

This paper is organized as follows. Section II presents the theory, which includes a description of the geometry of the plate and the estimation methodology. Section III is the numerical verification of proposed methodology. Experimental results are presented and discussed in Section IV, and concluding remarks are made in Section V.

II. THEORY

The primary effect of an applied load on guided wave propagation is a time shift Δt of a received guided wave signal, which is caused by both changes in phase velocity and dimensions of the plate. As is well-known for bulk wave acoustoelasticity [3], analysis can take place in either a *natural* coordinate system, where all spatial variables are measured relative to the unstressed material, or an *initial* coordinate system, where variables are relative to the stressed specimen. Here the natural system is convenient to use because the transducers are permanently affixed to the plate and in the natural system, the separation distance does not change. Thus, the change in phase velocity Δc_p in this natural system can be calculated from the measured time shift Δt as follows [19]:

$$\Delta c_p = -c_p^2 \frac{\Delta t}{d}. \tag{1}$$

Here c_p is the phase velocity at zero load and d is the distance between transducers in the natural coordinate system. In this paper, Eq. (1) is used to extract phase velocity changes from experimentally measured time shifts Δt.

To describe guided wave propagation in an aluminum plate of thickness h with biaxial applied stresses in the plane of the plate, a coordinate system is introduced as defined in Fig. 1. The unknown biaxial stresses σ_{11} and σ_{22} are assumed to be applied along the x_1 and x_2 axes of the rectilinear coordinate system x_i, from which a measurement coordinate system, indicated by x_i', is rotated by an angle α. It is further assumed that ultrasonic guided waves are propagating along a direction in the x_1-x_2 plane that makes an angle θ with respect to the x_1 axis and θ' with respect to the x_1' axis.

Gandhi *et al.* [19] have developed theory to calculate dispersion curves for Lamb wave propagation in prestressed plates with biaxial applied loads. Details of the theory are reported in [20]. Using software developed by Gandhi [20], dispersion curves for different propagating angles are plotted in Fig. 2(a) over a narrow frequency range for the S_0 fundamental guided wave mode, which illustrates the anisotropic effect caused by an applied anisotropic load. Fig. 2(b) shows changes of phase velocity with respect to propagation angle for this same mode and a frequency of 400 kHz. As noted by Gandhi [20], it can be seen that there is a sinusoidal relation between angle of propagation and change in phase velocity Δc_p.

Based on this sinusoidal dependence, equations that describe the relation between phase velocity change and propagation angle for uniaxial applied stresses at 0° and 90° have the following forms:

$$\Delta c_p(\theta)\Big|_{\sigma_{22}=0} = \sigma_{11}(K_1 \cos^2\theta + K_2 \sin^2\theta), \tag{2}$$

$$\Delta c_p(\theta)\Big|_{\sigma_{11}=0} = \sigma_{22}(K_3 \cos^2\theta + K_4 \sin^2\theta). \tag{3}$$

In these equations, Δc_p is the change of phase, θ is the direction of guided wave propagation in the principal (unprimed) coordinate system, and K_1, K_2, K_3 and K_4 are the four acoustoelastic constants for the particular frequency, mode and applied stress direction. Similar equations have been used for bulk and surface waves although the corresponding acoustoelastic constants are independent of frequency [3]. For an isotropic plate, the four acoustoelastic constants can be reduced to two (i.e., $K_1 = K_4$, $K_2 = K_3$) because of symmetry. We hypothesize that the linear combination of Eqs. (2) and (3) describes the change of phase velocity for an applied biaxial stress:

$$\Delta c_p(\theta) = (K_1\sigma_{11} + K_2\sigma_{22})\cos^2\theta + (K_2\sigma_{11} + K_1\sigma_{22})\sin^2\theta\,. \tag{4}$$

This equation is written in the unprimed coordinate system where the principal axes of the applied stress are aligned with the coordinate axes. However, measurements are made in the primed coordinate system, which is rotated by an angle α from the principal axis system. In this system, changes in phase velocity are,

$$\begin{aligned}\Delta c_p(\theta') &= (K_1\sigma_{11} + K_2\sigma_{22})\cos^2(\theta' + \alpha) + (K_2\sigma_{11} + K_1\sigma_{22})\sin^2(\theta' + \alpha) \\ &= a_0 + a_1\cos(2\theta') + a_2\sin(2\theta').\end{aligned} \tag{5}$$

The coefficients a_i are,

$$a_0 = \tfrac{1}{2}(K_1 + K_2)(\sigma_{11} + \sigma_{22})\,, \tag{6}$$

$$a_1 = \tfrac{1}{2}(K_1 - K_2)(\sigma_{11} - \sigma_{22})\cos(2\alpha)\,, \tag{7}$$

$$a_2 = -\tfrac{1}{2}(K_1 - K_2)(\sigma_{11} - \sigma_{22})\sin(2\alpha)\,. \tag{8}$$

These equations suggest a strategy to estimate the principal values and direction of the applied stresses. First, acoustoelastic constants K_1 and K_2 are estimated by least-squares from known uniaxial applied loads via Eq. (3) using measurements of phase velocity changes at multiple angles of propagation. Second, for similar measurements made at an unknown load, the coefficients a_0, a_1 and a_2 can be determined by least-squares using Eq. (5). Finally, the applied stresses σ_{11} and σ_{22} and the angle α are solved by inverting Eqs. (6), (7) and (8) for the unknown quantities:

$$\alpha = \frac{1}{2}\tan^{-1}\left(-\frac{a_2}{a_1}\right), \tag{9}$$

$$\sigma_{11} = \frac{a_0\cos(2\alpha)(K_1 - K_2) + a_1(K_1 + K_2)}{\cos(2\alpha)(K_1^2 - K_2^2)}, \tag{10}$$

$$\sigma_{22} = \frac{a_0\cos(2\alpha)(K_1 - K_2) - a_1(K_1 + K_2)}{\cos(2\alpha)(K_1^2 - K_2^2)}, \tag{11}$$

III. NUMERICAL VERIFICATION

The proposed strategy for estimating biaxial loads depends upon the hypothesis that changes in phase velocity due to a biaxial load are a linear combination of the two contributions for the uniaxial principal components. To verify this hypothesis, numerical simulations are performed to assess its validity. The changes of phase velocity at the 400 kHz for the S_0 mode of guided waves in a homogeneous and isotropic aluminum plate of thickness 3.175 mm were chosen to be consistent with the later experimental verification. The material properties of the plate for numerical simulation are described in Table 1. Note that the software calculates all phase velocity changes in the natural (unstressed) coordinate system.

First, phase velocity changes Δc_p were calculated for multiple uniaxial stress conditions as $\sigma_{11} = 0$ and σ_{22} increasing from 0 to 100 MPa in steps of 10 MPa; the propagation angle θ varied from 0 to 90 degrees in steps of 5 degrees. Second, acoustoelastic constants K_1 and K_2 were estimated by least-squares using Eq. (3) using the multiple known uniaxial stresses and corresponding phase velocity changes Δc_p obtained from the first step; their values were consistent for all loads considered. Third, theoretical phase velocity changes were calculated as a function of propagation angle for multiple cases of α, σ_{11} and σ_{22}. Finally, K_1 and K_2

determined from the second step were used in Eq. (5) to approximate the changes of phase velocity for the multiple cases of α, σ_{11} and σ_{22}.

The approximate results calculated as per Eq. (5) were found to be in excellent agreement with the theoretical phase velocity changes Δc_p for all cases considered. Typical results are shown in Fig. 3 for two cases: (1) $\alpha = 30°$, $\sigma_{11} = 50$ MPa, $\sigma_{22} = 100$ MPa, and (2) $\alpha = 90°$, $\sigma_{11} = 10$ MPa, $\sigma_{22} = 40$ MPa. The root mean square errors for these two cases are 0.0663m/s and 0.0112m/s, respectively, and are typical for all cases considered. Therefore, the assumed sinusoidal dependence and linear combination of uniaxial loads as expressed in Eqs. (4) and (5) are taken to be correct.

IV. EXPERIMENTS AND RESULTS

Fatigue tests were conducted for an array of six surface-bonded PZT transducers permanently attached to two different 6061 aluminum plates. Each transducer pair corresponds to guided wave propagation along a particular direction, which corresponds to the line connecting the transducers. Figures 4 and 5 show sketches of the transducer pattern and plate geometry for the two plates. Both specimens were fatigued using a 3 Hz sinusoidal tension-tension profile from 16.5 MPa to 165 MPa. Ultrasonic signals from the 15 unique transducer pairs were recorded for uniaxial loads ranging from 0 to 115 MPa in steps of 11.5 MPa as each data set. Several data sets were recorded during each fatigue test, where each data set contains 11 static loading measurements. Information about the crack growth in the two plates is summarized in Table 2.

Data were recorded by exciting each transducer in turn with a broadband chirp waveform, and the measured signals were filtered by a 7 cycle, Hanning windowed, 400 kHz tone burst signal as

described in [21]. The S_0 Lamb wave mode was chosen for analysis because it has clear first arrivals from all the transducer pairs and it is also the dominant mode at this frequency. The only other possible mode at 400 kHz is the slower A_0 mode, and the echoes were not sufficiently distinct to accurately extract phase velocity changes.

A. CALIBRATION AND ERROR ANALYSIS

The calibration procedure was performed to calculate the acoustoelastic constants K_1 and K_2 using data recorded from the first data set for both fatigue tests. Figure 6(a) shows the received S_0 signals from transducer pair 2-5 (i.e., transmitting on #2 and receiving on #5) of data set #1 from the first specimen at different loads. The zero crossings of these direct arrivals were extracted as a function of applied load and are plotted in Fig. 6(b); it can be seen that the small time shifts relative to zero load are linear with load over the entire load range. The corresponding changes of phase velocity Δc_p for the 11 loading conditions and 15 transducer pairs in data set #1 were calculated by Eq. (1) from the calculated time shifts, nominal values of c_p obtained at zero-load from dispersion curves, and measured transducer separation distances. The data of Δc_p calculated from all the transducer pairs were then used in Eq. (3) to estimate constants K_1 and K_2 from all known uniaxial loads via the best sinusoidal fit.

Figure 7 shows the sinusoidal fit for phase velocity changes Δc_p with respect to the angle of propagation for one specified load. To evaluate the fit, the root mean square (RMS) error between the experimental and fitted data as shown in Figure 7 was computed using the estimated values of K_1 and K_2 obtained from all of the uniaxial loads. The small value of 0.5037m/s indicates an excellent sinusoidal fit, and the corresponding values of K_1 and K_2 (-3.42×10^{-7} m/s/Pa and 0.69×10^{-7} m/s/Pa, respectively) are thus assumed to be accurate. The same

calibration procedure was applied to data set #1 of fatigue test 2, although the specimen during calibration was not pristine (the four holes were pre-drilled). The acoustoelastic constants K_1 and K_2 were found to be -3.77×10^{-7} m/s/Pa and 0.71×10^{-7} m/s/Pa, respectively, which are very close to those values calculated from the first specimen.

Once K_1 and K_2 are obtained, applied stresses and directions can be estimated from the phase velocity changes Δc_p obtained from later data sets using Eqs. (5), (9), (10) and (11). However, as the cracks grow in the plate and open under load, the received ultrasonic signals are affected by the guided waves interacting with and scattering from the cracks. As shown in Fig. 8 for transducer pair 2-5 of data set #9 from the first fatigue test, the relationship between time shift and applied load is no longer linear over the full range of applied loads. As the time shift data become skewed by the opening cracks, there are resulting errors in the phase velocity changes Δc_p. These errors affect the sinusoidal fit of Eq. (5) and subsequent determination of both the a_i and the recovered stress information.

To determine error bars for estimated stress results, consider the following least squares minimization based upon Eq. (5):

$$E = \sum_{i=1}^{N} \left\{ \Delta c_p(\theta_i') - \left[a_0 + a_1 \cos(2\theta_i') + a_2 \sin(2\theta_i') \right] \right\}^2 . \tag{12}$$

The resulting values of a_0, a_1 and a_2 can be expressed as a linear combination of the $\Delta c_p(\theta'_i)$, the change of phase velocity measured by the i*th* transducer pair:

$$\begin{bmatrix} a_0 \\ a_1 \\ a_2 \end{bmatrix} = \mathbf{C}^{-1} \begin{bmatrix} 1 & 1 & \cdots & 1 \\ \cos(2\theta_1') & \cos(2\theta_2') & \cdots & \cos(2\theta_N') \\ \sin(2\theta_1') & \sin(2\theta_2') & & \sin(2\theta_N') \end{bmatrix} \begin{bmatrix} \Delta c_p(\theta_1') \\ \Delta c_p(\theta_2') \\ \vdots \\ \Delta c_p(\theta_N') \end{bmatrix}, \tag{13}$$

where the **C** matrix is defined as [22],

$$\mathbf{C} = \begin{bmatrix} N & \sum_{i=1}^{N}\cos(2\theta_i') & \sum_{i=1}^{N}\sin(2\theta_i') \\ \sum_{i=1}^{N}\cos(2\theta_i') & \sum_{i=1}^{N}\cos^2(2\theta_i') & \sum_{i=1}^{N}\cos(2\theta_i')\sin(2\theta_i') \\ \sum_{i=1}^{N}\sin(2\theta_i') & \sum_{i=1}^{N}\cos(2\theta_i')\sin(2\theta_i') & \sum_{i=1}^{N}\sin^2(2\theta_i') \end{bmatrix}. \quad (14)$$

The variance associated with each a_j can then be calculated by:

$$\sigma^2(a_j) = \sum_{i=1}^{N}\sigma_i^2\left(\frac{\partial a_j}{\partial \Delta c_p(\theta_i')}\right)^2. \quad (15)$$

Here σ_i is the standard deviation of $\Delta c_p(\theta'_i)$, the change in phase velocity measured from the i*th* transducer pair. These standard deviations are all assumed to be equal, and are set to the sample standard deviation of the errors of $\Delta c_p(\theta'_i)$ from the sinusoidal fit performed for each unknown load. Thus, when there are no cracks and the fit is very good, the standard deviation is low, and as cracks grow and affect the guided wave signals, the fit becomes worse and the standard deviation increases.

Finally, the standard deviation of estimated stresses and directions are computed from the variance of parameters a_0, a_1 and a_2 as follows,

$$\sigma^2(\sigma_{nn}) = \sum_{j=0}^{2}\sigma^2(a_j)\left(\frac{\partial \sigma_{nn}}{\partial a_j}\right)^2 \text{ and } \sigma^2(\alpha) = \sum_{j=0}^{2}\sigma^2(a_j)\left(\frac{\partial \alpha}{\partial a_j}\right)^2. \quad (16)$$

This procedure was implemented for both fatigue tests to obtain error bars on final estimated results.

B. FATIGUE TEST 1 RESULTS

The eventual accuracy of the estimated loads is driven by the sinusoidal fit of $\Delta c_p(\theta_i)$. As was seen in Figure 7, this fit is typically very good when there are no cracks. In contrast, Figure 9 shows typical data from the first fatigue test for two different loads when cracks are present. If the data points (all solid and open circles) are compared to the sinusoidal fit (dashed lines), there are clearly significant errors for some of the data points. These errors are particularly large for transducer pairs whose path of direct propagation lies close to the site of cracking, as was shown in Figure 8.

To minimize the effects of opening cracks on stress estimates, data from some of the transducer pairs were eliminated. As shown in Fig. 4, it can be seen that the direct arrivals for three transducer pairs travelled directly through the cracked region: 1-4, 2-5, and 3-6. Data from these three pairs were excluded from the sinusoidal fit as shown by the solid line in Figure 9; the three excluded data points are denoted by open circles. The standard deviation of Δc_p was estimated from the errors relative to the sinusoidal fits, parameters a_0, a_1, and a_2 were calculated using Eq. (5), and σ_{11}, σ_{22} and α were calculated from Eqs. (9), (10) and (11). The corresponding errors were estimated for both cases (with and without eliminating data) using Eq. (16).

Figure 10 shows estimated principal stress components and direction plotted as a function of data set number. For Fig. 11(a), the actual values are σ_{11} = 0 MPa, σ_{22} = 46 MPa, and α = 0°; for Fig. 11(b) they are σ_{11} = 0 MPa, σ_{22} = 92 MPa, and α = 0°. It can be seen that elimination of the three transducer pairs reduces the impact of cracks and significantly improves the accuracy of the recovered values.

C. FATIGUE TEST 2 RESULTS

Another fatigue test was taken for the examination of the efficacy of the load estimation strategy using an aluminum plate with a different geometry as shown in Fig. 5. The distribution and growth of cracks in the specimen used in fatigue test 2 is much more complicated because the four holes provide additional sites of crack initiation. A total of eight cracks initiated and grew around the region of holes during the fatigue test. However, the same idea of eliminating transducer pairs whose paths intersected with cracks was still effective. The difference is that only the six transducer pairs corresponding to waves propagating near the periphery of the transducer polygon were used; the nine transducer pairs 1-4, 2-5, 3-6, 1-6, 3-4, 1-5, 3-5, 2-4 and 2-6 were eliminated. Figure 11 shows estimated loads and directions compared with actual applied stresses for two different loading cases. As expected, elimination of transducer pairs gives better results.

V. DISCUSSION AND CONCLUSIONS

Results from both fatigue tests show that the proposed method of estimating applied biaxial stresses from a spatially distributed array of guided wave transducers can provide accurate results when cracks are not present along the paths of propagation. As cracks grow and interfere with received signals, the accuracy of the estimates decreases, which is mitigated by removing some of the data. While the accuracy may not be as good as what can be achieved using, for example, dedicated strain gages, the method has the advantage of not requiring additional transducers.

This method is of particular interest for the case where a spatially distributed transducer array is attached on a plate-like structure since multiple transducer pairs correspond to guided waves

propagating at various angles. It can be used to estimate loads in conjunction with sparse array imaging of damage by using the same transducers and recorded signals. Measuring phase velocity changes Δc_p at multiple angles in the measurement coordinate system has the advantage of estimating the unknown direction of the applied stress, which cannot be achieved from measurements along a single direction. Furthermore, only two acoustoelastic constants are needed to estimate unknown applied stresses and directions, and these two constants can be estimated from a single uniaxial loading case.

Recommended future work includes performing experimental measurements incorporating true biaxial loads, and adapting the estimation strategy to anisotropic materials. It may also be possible to develop an algorithm to automatically mitigate the impact of cracks on ultrasonic signals when the locations of the cracks are unknown.

ACKNOWLEDGEMENTS

The authors gratefully acknowledge and appreciate the support of the Air Force Research Laboratory, Contract No. FA8650-09-C-5206 (program manager Mr. Charles Buynak), and the invaluable assistance of Mr. Xin Chen with the experiments.

REFERENCES

1. X. Chen, J. E. Michaels, S. J. Lee, and T. E. Michaels, "Load-differential imaging for detection and localization of fatigue cracks using Lamb waves," *NDT&E International*, under review, 2012.
2. D. S. Hughes and J. L. Kelly, "Second-order elastic deformation of solids," *Physical Review Letter*, **92**(5), pp. 1145-1149, 1953.
3. Y. H. Pao, W. Sachse and H. Fukuoka, "Acoustoelasticity and ultrasonic measurement of residual stresses," *Physical Acoustics*, **XVII**, pp. 63-143, 1984.

4. Y. H. Pao, T. T. Wu and U. Gamer, "Acoustoelastic birefringences in plastically deformed solids," *Journal of Applied Physics*, **58**(1), pp. 11-17, 1991.

5. A. D. Degtyar and S. I. Rokhlin, "Absolute stress determination in orthotropic materials from angular dependence of ultrasonic velocities," *Journal of Applied Physics*, **78**(3), pp. 1547-1556, 1995.

6. T. Berruti, M. M. Gola and G. A. D. Briggs, "Acoustoelastic measurement on aluminum alloy by means of a contact and a non-contact (LFB acoustic microscopy)," *Journal of the Acoustical Society of America*, **103**(3), pp. 1370-1376, 1998.

7. M. Duquennoy, M. Quaftouh, M. Ourak and F. Jenot, "Theoretical determination of Rayleigh wave acoustoelastic coefficients: comparison with experimental values," *Ultrasonics*, **39**, pp. 575-593, 2002.

8. M. Duquennoy, M. Quaftouh, M. Ourak, D. Lochegnies and E. Romero, "Ultrasonic evaluation of residual stresses in flat glass tempering: Comparing experimental investigation and numerical modeling," *Journal of the Acoustical Society of America*, **119**(6), pp. 3773-3781, 2006.

9. M. Junge, J. Qu and L. J. Jacobs, "Relationship between Rayleigh wave polarization and state of stress," *Ultrasonics*, **44**, pp. 233-237, 2006.

10. P. Rizzo and F. Lanza di Scalea, "Effect of frequency on the acoustoelastic response of steel bars," *Experimental Techniques*, **27**(6), pp. 40-43, 2003.

11. F. Chen and P. D. Wilcox, "The effects of load on guided wave propagation," *Ultrasonics*, **47**(1-4), pp. 111-122, 2007.

12. P. W. Loveday and P. D. Wilcox, "Guided wave propagation as a measure of axial loads in rails," *Proceedings of SPIE, Health Monitoring of Structural and Biological Systems*, **7650**, T. Kundu (Ed.), SPIE, pp. 765023(8 pages), 2010.

13. S. Chaki and G. Bourse, "Guided ultrasonic waves for non-destructive monitoring of the stress levels in prestressed steel strands," *Ultrasonics*, **49**(2), pp. 162-171, 2009.

14. I. Bartoli, C. Nucera, A. Srivastava, S. Salamone, R. Phillips, F. Lanza di Scalea, S. Coccia and C. S. Sikorsky, "Nonlinear ultrasonic guided waves for stress monitoring in prestressing tendons for post-tensioned concrete structures," *Proceedings of SPIE, Health Monitoring of Structural and Biological Systems*, **7292**, T. Kundu (Ed.), SPIE, pp. 729220(11 pages), 2009.

15. C. Desmet, U. Kawald, A. Mourad, W. Lauriks and J. Thoen, "The behavior of Lamb waves in stressed polymer foils," *Journal of the Acoustical Society of America*, **100**(3), pp. 1509-1531, 1996.

16. M. Lematre, G. Feuillard, T. Delaunay and M. Lethiecq, "Modeling of ultrasonic wave propagating in integrated piezoelectric structures under residual stress," *IEEE Transaction on Ultrasonics, and Frequency Control*, **53**(4), pp. 685-696, 2006.

17. A. Zagrai, V. Gigineishvili, W. A. Kruse, A. Murray, D. Doyle, W. Reynolds, B. Arritt and H. Gardenier, "Acousto-Elastic measurements and baseline-free assessment of bolted joints using guided waves in space structures," *Proceedings of SPIE, Health Monitoring of Structural and Biological Systems*, **7650**, T. Kundu (Ed.), SPIE, pp. 765017(12 pages), 2010.

18. F. Shi, J. E. Michaels and S. J. Lee, "An ultrasonic guided wave method to estimate applied biaxial loads," *Review of Progress in Quantitative Nondestructive Evaluation*, **31**, in press, expected 2012.

19. N. Gandhi, J. E. Michaels and S. J. Lee, "Acoustoelastic Lamb wave propagation in a homogeneous, isotropic aluminum plate," *Review of Progress in Quantitative Nondestructive Evaluation*, **30**, pp. 161-168, 2011.

20. N. Gandhi, *Determination of Dispersion Curves for Acoustoelastic Lamb Wave Propagation*, M.S. Thesis, Georgia Institute of Technology, 2010.

21. J. E. Michaels, S. J. Lee, J. S. Hall and T. E. Michaels, "Multi-mode and multi-frequency guided wave imaging via chirp excitations," *Proceedings of SPIE, Health Monitoring of Structural and Biological Systems*, **7984**, T. Kundu (Ed.), SPIE, pp. 79840I (11 pages), 2011.

22. W. H. Press, S. A. Teukolsky, W. T. Vetterling and B. P. Flannery, *Numerical recipes 3rd edition: The art of scientific computing*, Cambridge University Press, pp. 773-839, 2007

Table 1. Density and elastic constants of aluminum used for simulations.

Property	Value and Units
ρ	2700 kg/m^3
λ	50.281 GPa
μ	25.902 GPa
l	-252.2 GPa
m	-324.9 GPa
n	-351.2 GPa

Table 2. Descriptions of crack growth during the two fatigue tests.

Data Set	Fatigue Test 1		Fatigue Test 2	
	Fatigue Cycles	Notes Largest Crack	Fatigue Cycles	Notes Largest Crack
1	0	Pristine plate	0	4 holes
2	0	Starter hole	0	4 holes, 2 notches
3	0	Hole with notch	2,000	0.7 mm
4	5,000	0	2,500	1.3 mm
5	8,000	1.6 mm	3,000	1.8 mm
6	10,000	3.6 mm	3,500	2.0 mm
7	12,500	5.4 mm	5,500	4.3 mm
8	15,500	7.7 mm	6,500	4.9 mm
9	17,000	9.9 mm	7,000	5.4 mm
10	18,500	13.4 mm	7,500	6.4 mm
11	19,500	16.8 mm	8,500	8.4 mm
12	20,000	19.5 mm	9,500	10.5 mm
13	20,400	22.7 mm	10,400	13.0 mm
14	20,600	25.2 mm	---	---

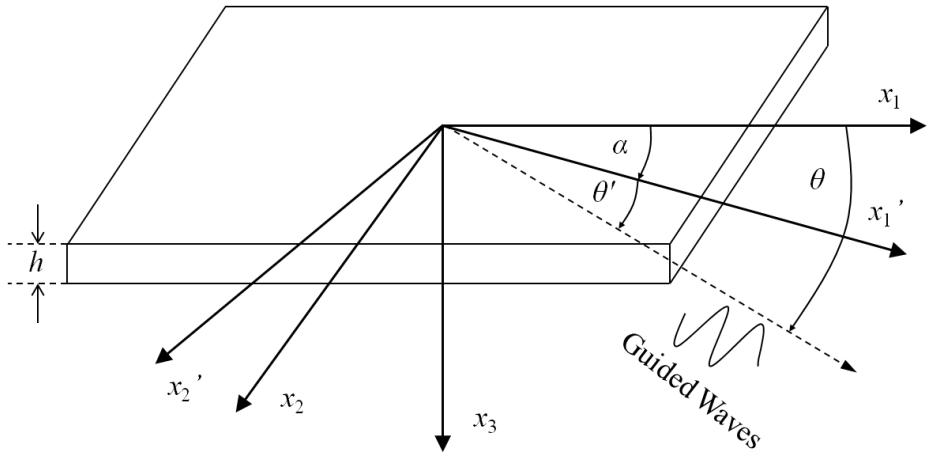

Figure 1. Geometry for guided wave propagation in a prestressed aluminum plate.

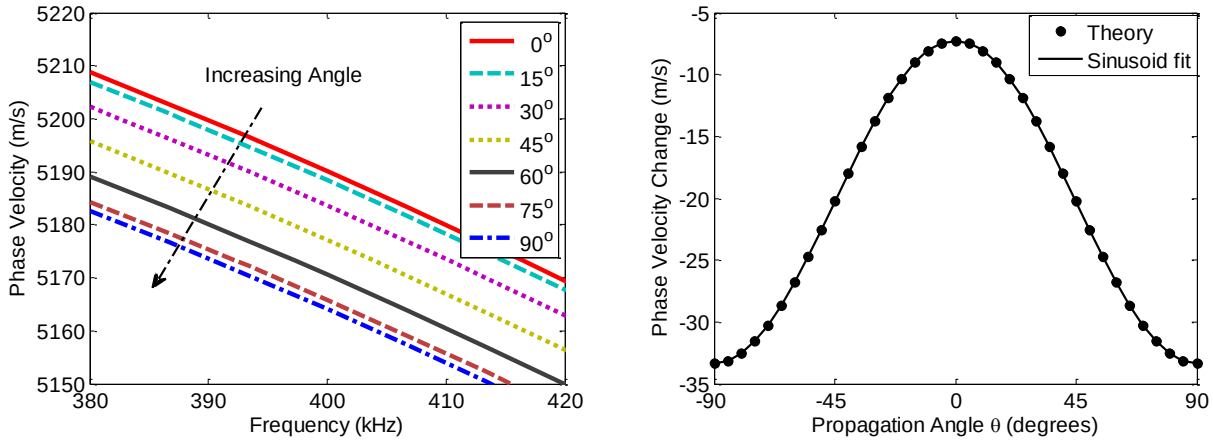

(a) (b)

Figure 2. (a) Dispersion curves for the S_0 mode at different propagation angles when σ_{11} = 30 MPa and σ_{22} = 80 MPa. (b) Changes of phase velocity for the S_0 mode at 400 kHz as a function of propagation angle when σ_{11} = 30 MPa and σ_{22} = 80 MPa.

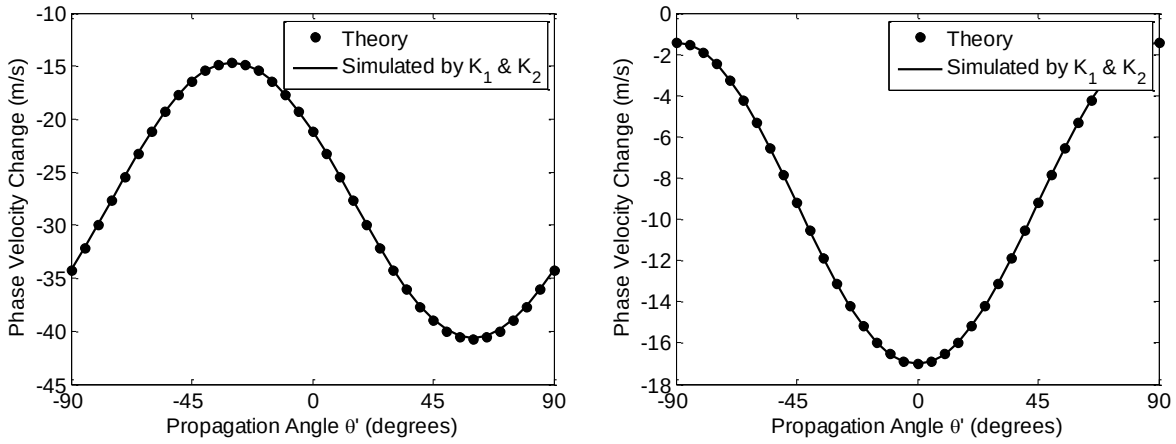

(a) (b)

Figure 3. Phase velocity changes for the S_0 mode at 400 kHz versus propagation angle for different applied loads. (a) σ_{11} = 50 MPa, σ_{22} = 100 MPa, and α = 30 degrees. (b) σ_{11} = 10 MPa, σ_{22} = 40 MPa, and α = 90 degrees.

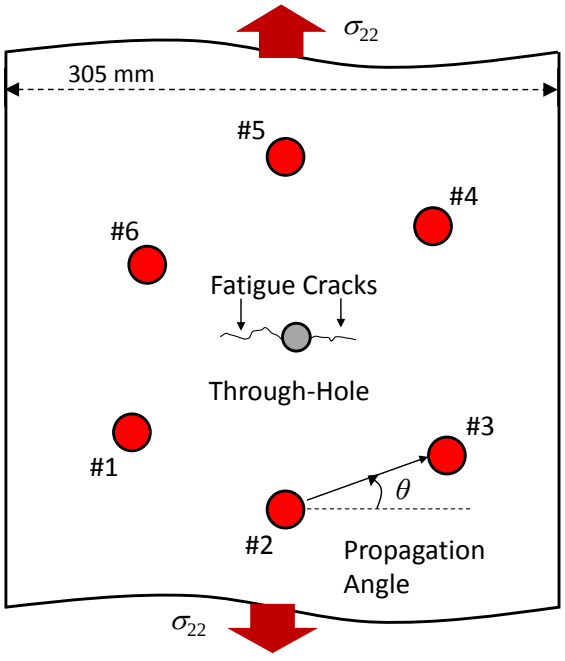

Figure 4. Drawing of the specimen and transducer geometry for fatigue test 1 (not to scale).

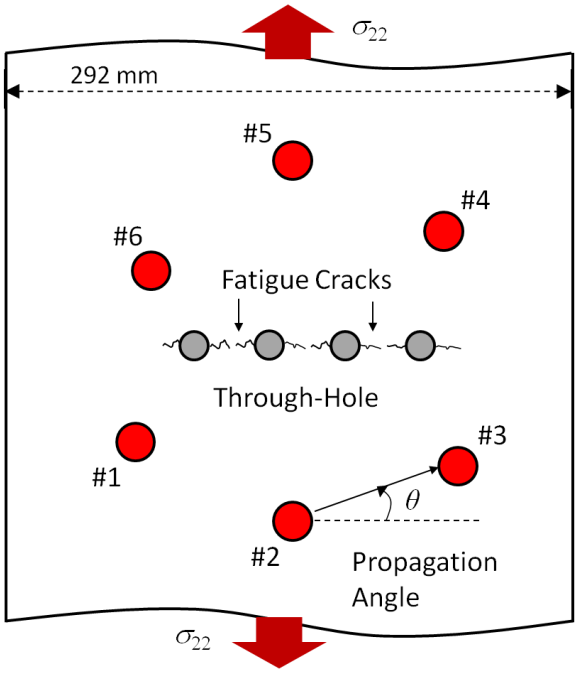

Figure 5. Drawing of the specimen and transducer geometry for fatigue test 2 (not to scale).

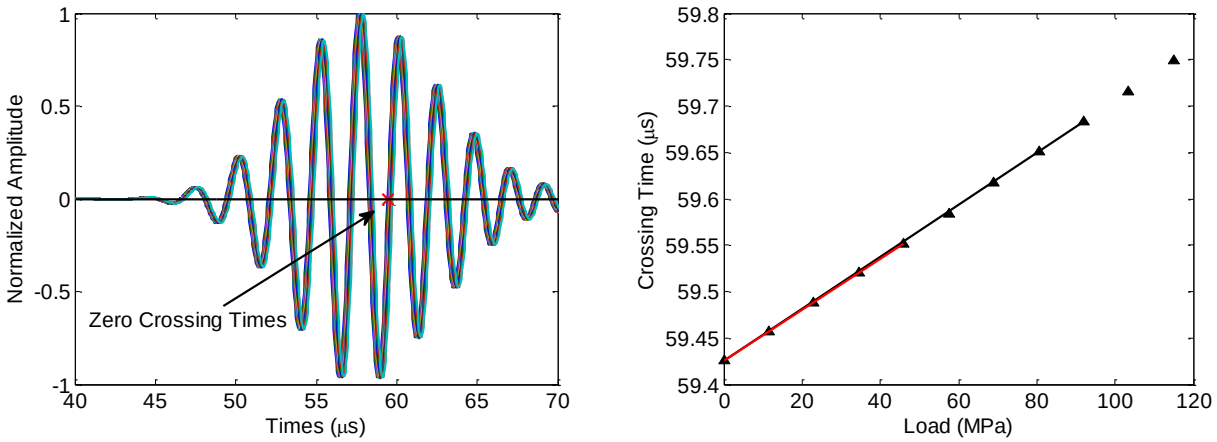

(a) (b)

Figure 6. (a) First arrivals of transducer pair 2−5, data set #1 (no holes, no cracks) of fatigue test 1, for all 11 uniaxial loading conditions. (b) Zero crossing times with respect to loads for transducer pair 2−5, data set #1.

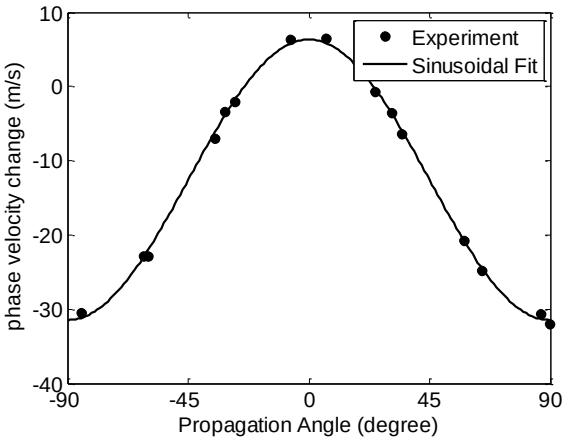

Figure 7. Experimental data and sinusoidal fit of phase velocity changes versus angle for data set 1 of fatigue test 1 when σ_{11} = 0 MPa, σ_{22} = 92 MPa.

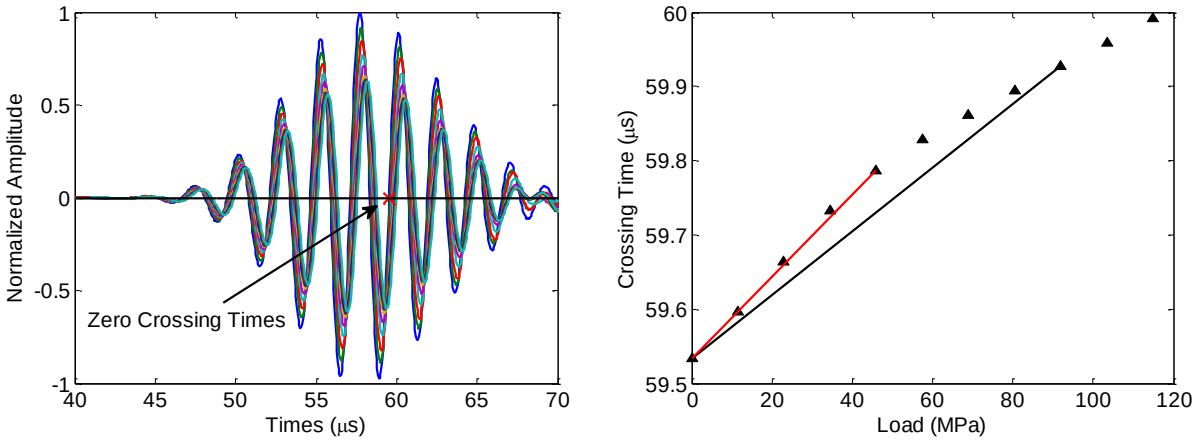

Figure 8. (a) First arrivals of transducer pair 2−5, data set #9, fatigue test 1, for all 11 uniaxial loading conditions. (b) Zero crossing times with respect to loads for transducer pair #2−5, data set #9

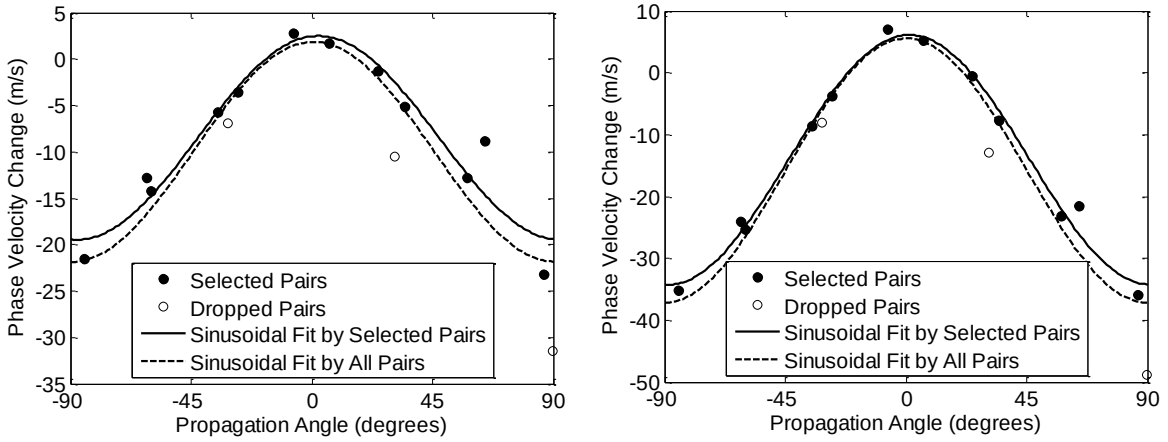

Figure 9. Experimental data and sinusoidal fit of phase velocity changes versus angle for data set #9. (a) σ_{11} = 0 MPa, σ_{22} = 46 MPa, (b) σ_{11} = 0 MPa, σ_{22} = 92 MPa

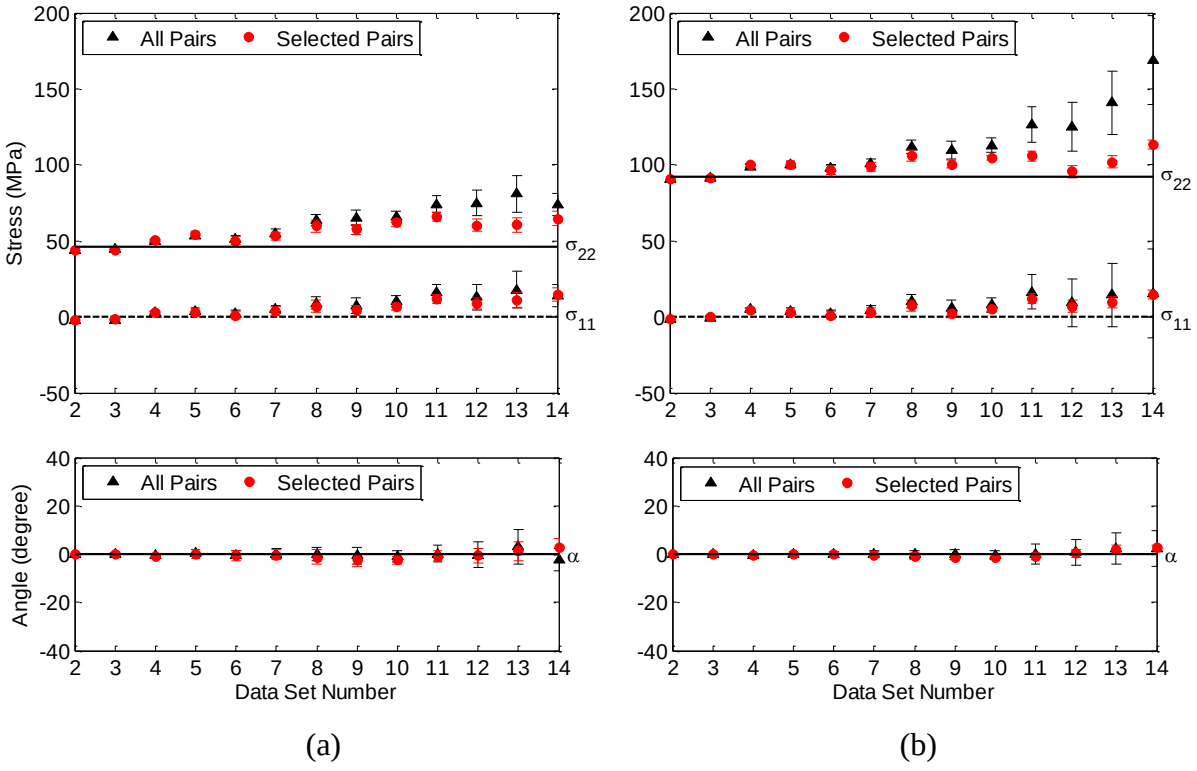

Figure 10. Estimated stresses and orientation angles for all data sets of fatigue test 1. (a) σ_{11} = 0 MPa, σ_{22} = 46 MPa, α = 0°. (b) σ_{11} = 0 MPa, σ_{22} = 92 MPa, α = 0°.

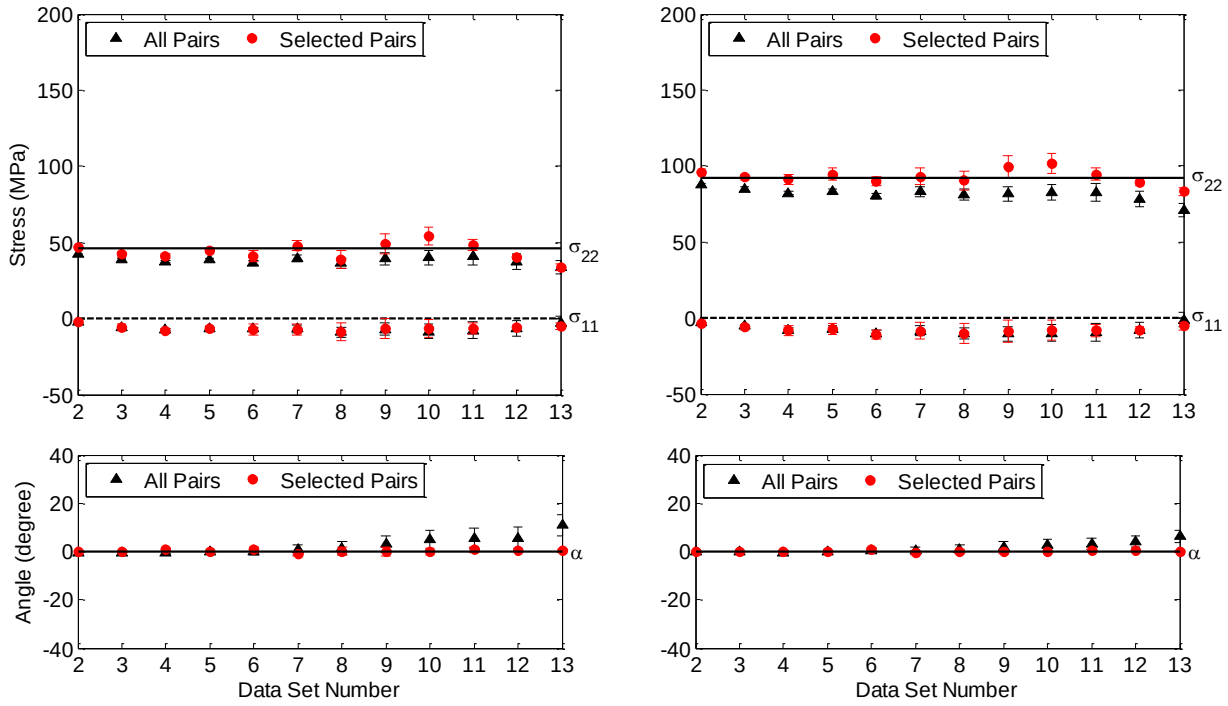

Figure 11. Estimated stresses and orientation angles for all data sets of fatigue test 2. (a) σ_{11} = 0 MPa, σ_{22} = 46 MPa, α = 0°. (b) σ_{11} = 0 MPa, σ_{22} = 92 MPa, α = 0°.